OPEN ACCESS
JOURNAL OF ADVANCED DIELECTRICS
Vol. 11, No. 1 (2021) 2150007 (8 pages)

DOI: 10.1142/S2010135X21500077

Dielectric properties and electrical response of yttrium-doped $Bi_{2/3}Cu_3Ti_4O_{12}$ ceramics

Longhai Yang*,§, Luwen Song*, Qi Li† and Tao Zhang‡

*School of Electrical and Control Engineering
Xi'an University of Science and Technology
Xi'an 710054, Shaanxi, P. R. China

†School of Materials Science and Engineering
Shaanxi Normal University, Xi'an 710062, Shaanxi, P. R. China

‡School of Science, Xi'an University of Science and Technology
Xi'an 710054, Shaanxi, P. R. China

§ylonghai@hotmail.com

Received 21 October 2020; Revised 10 February 2021; Accepted 11 February 2021; Published 26 February 2021

$(Y_xBi_{1-x})_{2/3}Cu_3Ti_4O_{12}$ (x=0.00–0.30) ceramics were successfully prepared via the conventional solid-state method. X-ray powder diffraction confirmed the lattice constant gradually decreases with increasing Y^{3+} content. SEM images displayed Y^{3+} substitution for Bi^{3+} gave rise to the large abnormal grains, and the size of abnormal grains became larger with the increase of Y^{3+} substitution. $(Y_xBi_{1-x})_{2/3}Cu_3Ti_4O_{12}$ ceramics presented the relatively high dielectric constant of 7400 with the dielectric loss of 0.055 when x = 0.20. The analysis of complex impedance suggested the grains are semiconductive and the grain boundaries are insulating. For pure $Bi_{2/3}Cu_3Ti_4O_{12}$ ceramics, the appearance of additional low-frequency peaks in electrical modulus indicated the grain boundaries are heterogeneous. The investigation of modulus peaks fitting with Arrhenius formula implied that the low-frequency permittivity for all $(Y_xBi_{1-x})_{2/3}Cu_3Ti_4O_{12}$ ceramics was ascribed to the Maxwell–Wagner relaxation at grain boundaries. In addition, a set of clear dielectric peaks above 200 °C associated with Maxwell–Wagner relaxation can be found for all $(Y_xBi_{1-x})_{2/3}Cu_3Ti_4O_{12}$ ceramics in the temperature dependence of dielectric constant. This set of clear dielectric peaks showed a tendency to shift to higher temperatures with the increase of Y^{3+} substitution. Meanwhile, a tiny dielectric anomaly at room temperature was found in Y-doped $Bi_{2/3}Cu_3Ti_4O_{12}$ ceramics.

Keywords: Ceramics; microstructure; dielectric properties; impedance spectroscopy.

1. Introduction

Over the past few years, much attention has been paid to $CaCu_3Ti_4O_{12}$ (CCTO) ceramics in view of its giant dielectric permittivity (10^4 to 10^5) over the frequency range from DC to 1 MHz and also, its giant permittivity is independent of temperature within a temperature range of 100–400 K, which suggests the potential application in capacitor-based devices.[1–5] $Bi_{2/3}Cu_3Ti_4O_{12}$ (BCTO), as a member of CCTO-like compounds with a compositional formula of $ACu_3Ti_4O_{12}$-(A = Sr, $Bi_{2/3}$, $Bi_{1/2}Na_{1/2}$, $La_{2/3}$, etc.), is isostructural with CCTO.[6–10] The previous investigations on BCTO primally focused on the preparation process and the origin of the giant permittivity.[10–14] Through a traditional solid-state technique, a low-frequency dielectric constant of ~2000 was obtained. It exhibited the same temperature and frequency dependence of the dielectric behavior as CCTO and explained its dielectric constant as arising from Maxwell–Wagner relaxation occurring at the interfaces of grains and grain boundaries.[10] Moreover, a very large low-frequency dielectric constant (150,000) of BCTO ceramics was obtained through conventional solid-state reaction accompanied with a rapid cooling temperature process. The comparison experiment of different electrodes illustrated this large value was attributed to electrode effect.[11] Furthermore, a relatively high permittivity of ~12,000 was obtained by sol–gel method.[12]

Recently, an investigation on Na^+ substitution for Bi^{3+} in $Bi_{2/3}Cu_3Ti_4O_{12}$ ceramics has been reported.[13] This nonequivalence substitution gave rise to variation in amount of A-site vacancies. The microstructure, dielectric properties, and complex impedance have been systematically investigated. The results indicate this nonequivalence substitution has a significant influence on the microstructure and electrical properties of BCTO ceramics. In order to further study the valence influence on the dielectric properties of $Bi_{2/3}Cu_3Ti_4O_{12}$, an equivalence substitution at A-sites was designed. $Y_{2/3}Cu_3Ti_4O_{12}$, which is also isostructural with CCTO, exhibited an outstanding dielectric property. Ceramics sintered at 1010 °C displayed a dielectric constant of ~11,000 and a dielectric loss of 0.033.[15]

§Corresponding author.

In addition, the ionic radius of Y^{3+} is larger than that of Bi^{3+}. The Y^{3+} substitution for Bi^{3+} in BCTO ceramics may change the degree of lattice distortion. Therefore, it is expected that Y^{3+} substitution for Bi^{3+} will affect the microstructure and dielectric properties of $Bi_{2/3}Cu_3Ti_4O_{12}$ ceramics.

Thus, based on the above analysis, a small amount of Y^{3+} substitution for Bi^{3+} has been carried out in $Bi_{2/3}Cu_3Ti_4O_{12}$ ceramics in the present work. The crystalline structure, microstructure, dielectric properties, and complex impedance were systematically investigated. In addition, high-temperature dielectric anomalies were discussed as well.

2. Experimental Procedure

$(Y_xBi_{1-x})_{2/3}Cu_3Ti_4O_{12}$ (x = 0.00, 0.10, 0.20, 0.25, 0.30, hereafter referred as YBCTO) ceramics were prepared by a conventional solid-state reaction technique. The stoichiometric amounts of highly pure Y_2O_3 (99.99%), Bi_2O_3 (99.0%), CuO (99%), TiO_2 (99.99%) were mixed and ball-milled in ethanol for 10 h. Subsequently, the mixtures were dried and calcined at 800 °C for 10 h in air. The calcined powders were blended with approximately 5 wt.% polyvinyl alcohol (PVA) and pressed into disk pellets (15 mm diameter and 1.5 mm in thickness) with a uniaxial pressure of 100 MPa after sufficient grounding. These disk pellets were sintered at 1000–1020 °C for 20 h in air. For electrical characterization, the sintered disk pellets were polished and then coated with silver paint and fired at 840 °C for 30 min.

The phase structures of the sintered specimens were identified by X-ray diffraction (XRD, D/max-2550/PC, Rigaku, Japan) with Cu K radiation and the microstructures were studied by scanning electron microscope (SEM, Quanta 200, Philips, Netherlands). Dielectric spectra and complex impedance at room temperature were measured by Agilent 4294A precise impedance analyzer within the frequency range of 40 Hz to 110 MHz. The measurement of dielectric properties with varied temperatures was carried out with the LCR meter (Agilent E4980A)

3. Results and Discussion

Figure 1 illustrates the X-ray diffraction patterns of YBCTO ceramics. All diffraction peaks agree with the cubic perovskite structure. Every composition exhibits the pure phase

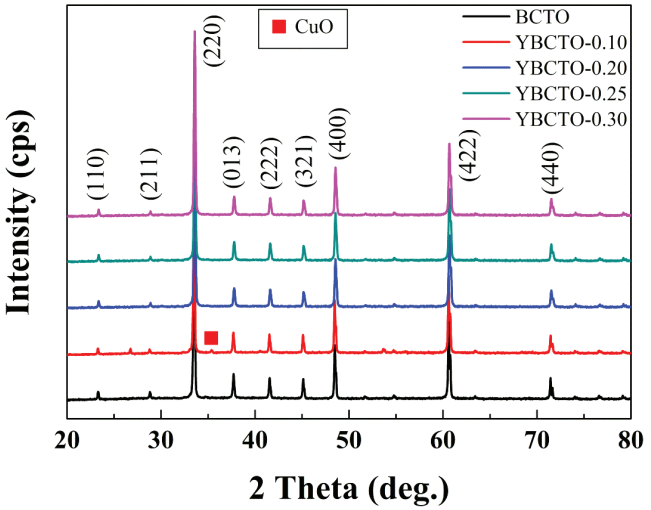

Fig. 1. XRD patterns for YBCTO ceramics.

structure with the exception of x = 0.1 samples, for which weak diffraction peaks at ~36° that corresponds to CuO can be observed. Through Pawley refinement conducted by TOPAS-Academic software, the lattice constant and theoretical density of $(Y_xBi_{1-x})_{2/3}Cu_3Ti_4O_{12}$ ceramics were calculated. As shown in Table 1, the lattice constant gradually decreases with increasing Y^{3+} content, which is due to the smaller ionic radius of Y^{3+} (r = 0.9 Å) compared to that of Bi^{3+} (r = 1.03 Å).

Figure 2 shows SEM images of YBCTO ceramics. For undoped BCTO ceramics, uniformly distributed grains with the size of 2–3 μm are observed, which are consistent with values in some reports.[10–13] For x = 0.10~0.30, the large abnormal grains appear. Some densely small grains are located around these large abnormal grains. With the increase of Y^{3+} substitution, the size of abnormal grains will increase but, the size of small grains is unchanging. It remains in the size of ~5 μm. The evolution of microstructure in the YBCTO ceramics is related to the variation of Bi_2O_3 content. As a kind of sintering aids, Bi_2O_3 solid state will be transformed into Bi_2O_3 liquid phase during the sintering. Fine grains are easily formed in the liquid phase when samples are cooling down. Thus, the less Bi_2O_3 content are, the larger the grains are. This view is also confirmed by the microstructure evolution of $Na_xBi_{(2-x)/3}Cu_3Ti_4O_{12}$ ceramics in which Bi^{3+} is substituted by Na^+.[13]

Table 1. Lattice constant and density of $(Y_xBi_{1-x})_{2/3}Cu_3Ti_4O_{12}$ ceramics.

Composition (x)	0.00	0.10	0.20	0.25	0.30
Lattice constant (Å)	7.4150 (1)	7.4112 (1)	7.4108 (1)	7.4024 (6)	7.3982 (4)
Theoretical density (g/cm^3)	5.81	5.76	5.69	5.66	5.73
Measured density (g/cm^3)	5.29	5.08	4.84	4.97	4.87
Relative density	91.0%	88.2%	85.1%	87.8%	85.0%

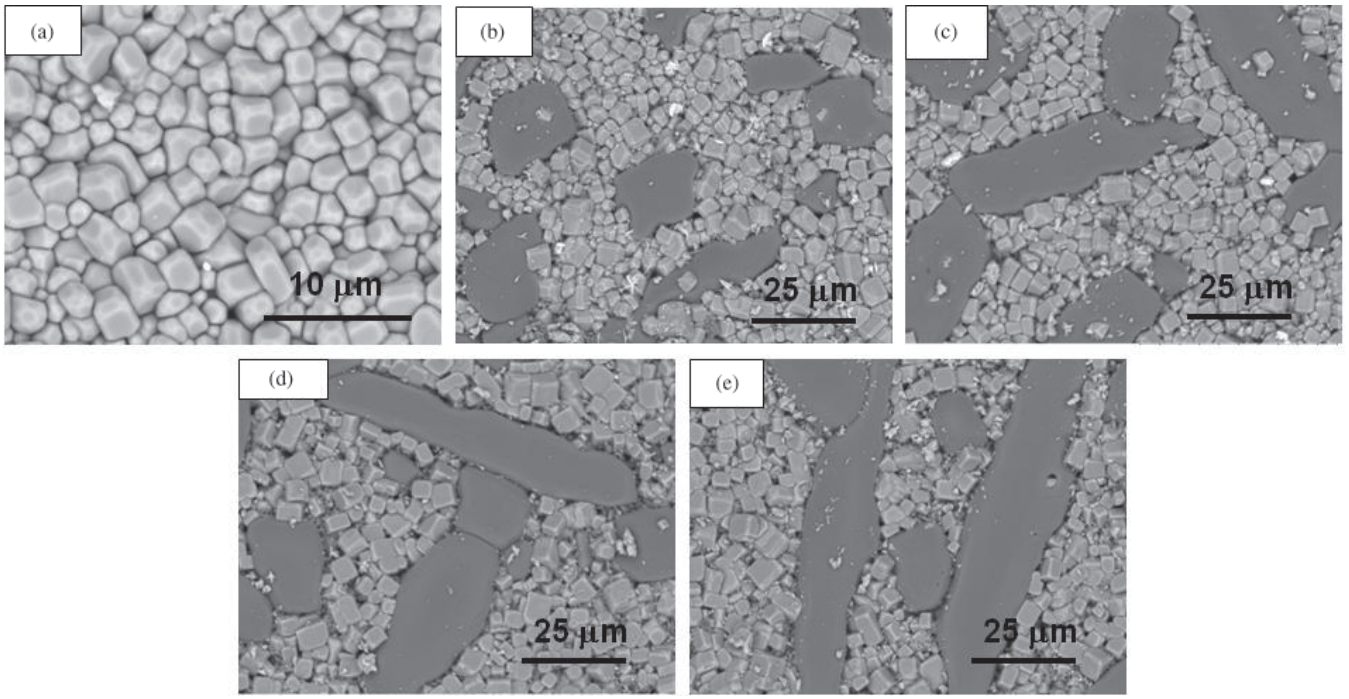

Fig. 2. SEM images for YBCTO ceramics. (a) BCTO, (b) YBCTO-0.10, (c) YBCTO-0.20, (d) YBCTO-0.25, (e) YBCTO-0.30.

Figure 3 exhibits the frequency dependence of dielectric constant and dielectric loss of YBCTO ceramics at room temperature in the frequency range from 40 Hz to 110 MHz. As shown in Fig. 3(a), the dielectric constant is about 2800 over the frequency range from 40 Hz to 100 kHz for undoped BCTO ceramics, which is close to these values reported in the literatures.[10,13] With the increase of Y^{3+} substitution, the permittivity first increases, which reaches maximum value of ~7400 when $x = 0.20$. With the Y^{3+} content further increasing, the permittivity decreases. The value of dielectric constant for YBCTO ceramics with $x = 0.30$ becomes very small, which is even lower than the permittivity of pure BCTO ceramics. Unfortunately, doping Y^{3+} is unable to lower the dielectric loss. Figure 4 shows the Y^{3+} content dependence of dielectric constant and dielectric loss at 1 kHz. Through the observation, an optimum composition of $x = 0.20$ was selected. YBCTO ceramics with $x = 0.20$ exhibits a high permittivity of ~ 7400 and a relatively low loss of ~ 0.055.

In order to explain the variation of dielectric properties caused by different Y^{3+} substitutions, the complex impedance plots of YBCTO ceramics at room temperature are shown in Fig. 5(a). Two obvious semicircular arcs in the complex impedance plane are observed for all samples, suggesting that YBCTO ceramics are electrically heterogeneous. The Z View Software was used to analyze impedance data. Figure 5(b) displays the fitting plot of complex impedance for pure BCTO ceramics at room temperature. The equivalent circuit mode consisting of two parallel resistor-constant phase angle element (R-CPE) elements was selected to simulate impedance, of which one R-CPE components is corresponding to the semiconducting region and the other one is corresponding to insulating region. It is found that the experimental result is in good consistent with the fitting data obtained from ZView analysis. Through fitting the complex impedance according to the equivalent circuit, the grains resistances Rg and grain boundaries resistances Rgb of YBCTO ceramics at room temperature are calculated, which are presented in Table 2. It is confirmed that grains are semiconductive and grain boundaries are insulating. This is well consistent with the internal barrier layer capacitor (IBLC) model.

In order to clarify the essential mechanism of variation in dielectric properties for YBCTO ceramics, electric modulus formalism of dielectric properties was used. Complex modulus M^* is defined as $1/\varepsilon^*$, where ε^* is complex permittivity,[16]

$$M^* = 1/\varepsilon^* = 1/(\varepsilon' - i\varepsilon'') = \varepsilon'/(\varepsilon'^2 + \varepsilon''^2) + i\varepsilon''/(\varepsilon'^2 + \varepsilon''^2) = M' + iM'', \quad (1)$$

where $M' = \varepsilon'/(\varepsilon'^2 + \varepsilon''^2)$ and $M'' = \varepsilon''/(\varepsilon'^2 + \varepsilon''^2)$ are the real and imaginary parts of complex modulus. The peak intensity of M'' is proportional to the reciprocals of the associated capacitances.[17] Figure 6 shows the frequency dependence of electric modulus for YBCTO ceramics at different temperatures. The measuring frequency range is from 40 Hz to 1 MHz. As shown in Fig. 6, only a set of modulus peaks can be observed for all samples. With the increase of temperature, the peak will shift to higher frequencies, indicating a thermally activated mechanism. For undoped BCTO ceramics and YBCTO ceramics with $x = 0.10$, the modulus peaks move into the measuring frequency window above 100 °C,

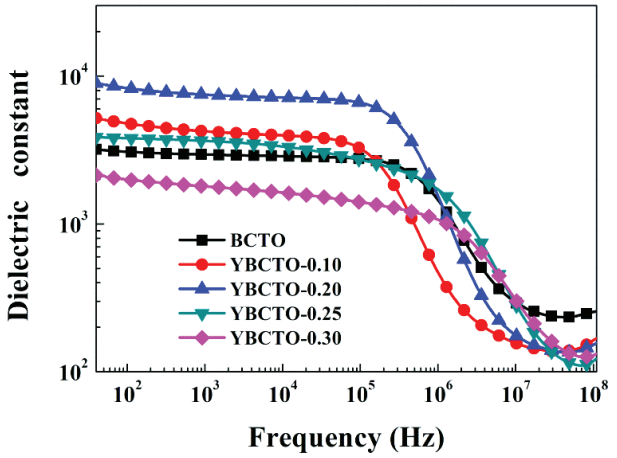

(a)

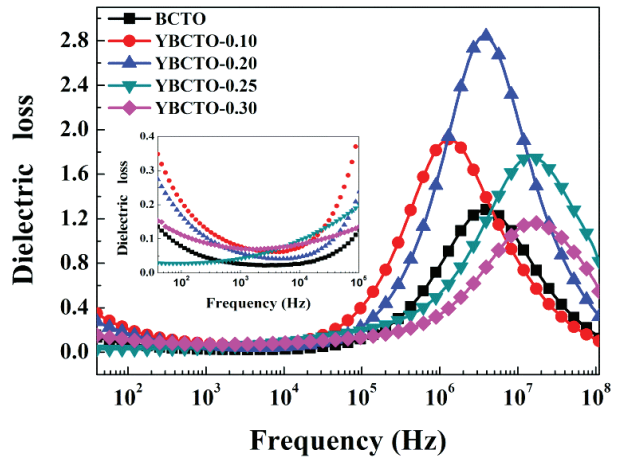

(b)

Fig. 3. Frequency dependence of dielectric constant (a) and dielectric loss (b) for YBCTO ceramics at room temperature.

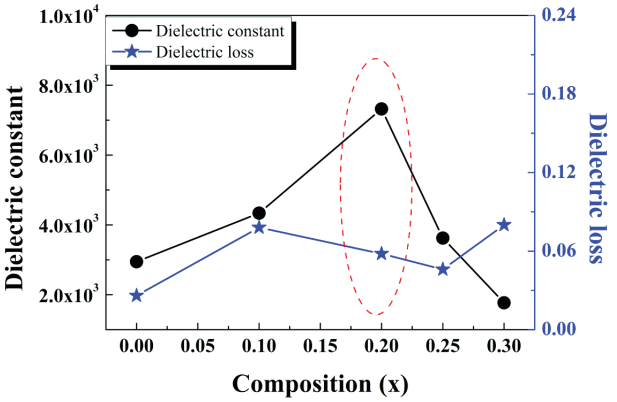

Fig. 4. Y^{3+} contents dependence of dielectric constant and dielectric loss.

while, for YBCTO ceramics with $x = 0.20$, 0.25 and 0.30, the modulus peaks can be observed in the measuring frequency range above 120 °C.

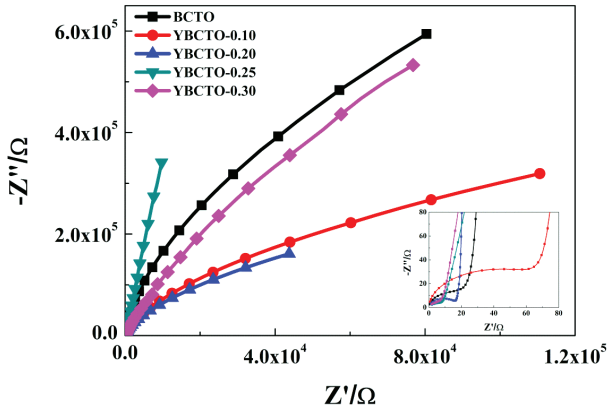

(a)

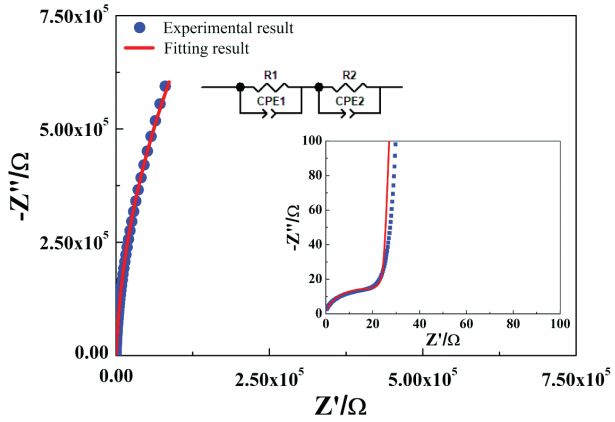

(b)

Fig. 5. (a) Complex impedance plots for YBCTO ceramics at room temperature, the inset shows an expanded view of the high frequency date close to the origin. (b) The fitting plot of complex impedance for BCTO ceramics at room temperature.

For all samples, the electric modulus peak can be well identified. The frequencies and temperatures of modulus peaks follow the Arrhenius law[18]

$$f_p = f_0(-E_a/k_BT) \quad (1)$$

where f_p is the peak frequency, f_o is the pre-exponential term, E_a is the activation energy, and K_B is the Boltzmann constant. The Arrhenius law fitting results for all samples are given in Fig. 7. For undoped BCTO ceramics, the activation energy E_a is 0.538 eV, which is lower than the value of 0. 70 eV.[10,12] For YBCTO ceramics with $x = 0.10$, the activation energy E_a goes up to 0.552 eV. With the Y^{3+} substitution further increasing, the activation energy E_a will decrease. The value of activation energy is down to 0.502 eV when $x = 0.30$. Overall, these values are well consistent with the value of 0.542 eV for the Maxwell–Wagner relaxation associated with grain boundaries in CCTO ceramics.[19] Therefore, it is concluded that the low-frequency dielectric permittivity for all samples is attributed to the Maxwell–Wagner relaxation associated with

Table 2. Grains resistances and grain boundaries resistances of $(Y_xBi_{1-x})_{2/3}Cu_3Ti_4O_{12}$ ceramics at room temperature.

Composition (x)	0.00	0.10	0.20	0.25	0.30
Rg (Ω)	24.49	67.04	17.12	9.54	9.74
Rgb (Ω)	5.29×10^6	1.10×10^6	6.49×10^5	9.66×10^6	9.32×10^6

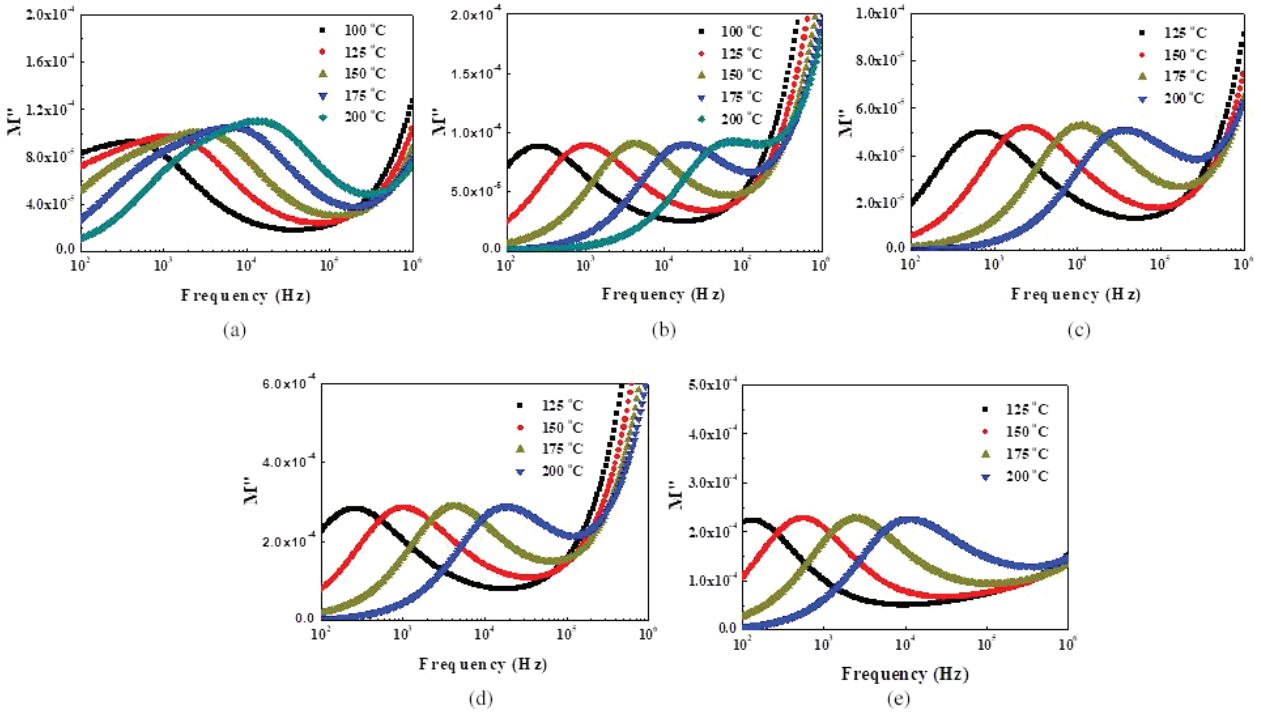

Fig. 6. Frequency dependence of electric modulus for YBCTO ceramics at different temperatures. (a) BCTO, (b) YBCTO-0.10, (c) YBCTO-0.20, (d) YBCTO-0.25, (e) YBCTO-0.30.

grain boundaries. The mechanism for giant low-frequency permittivity is unchanged during Y^{3+} substitution process.

For pure BCTO ceramics, in addition to the obvious peaks, a set of additional M'' peaks marked by red circle was found in electrical modulus. As shown in Fig. 8, the frequency of the additional modulus peak is lower than that of obvious modulus peaks for different temperature curves. It has been known that the obvious high frequency peaks in M'' was corresponding to the grain boundaries response through calculating the active energy. In the complex impedance in Fig. 5, through fitting impedance spectrum, there are two different electrical responses present in pure BCTO ceramics. The low-frequency arc corresponds to the grain boundary response and the high frequency arc corresponds to the grain response. No new electrical response is found in the whole frequencies range. Thus, the additional peaks found in low-frequency modulus may not be a definite individual response compared to the grain boundary and bulk response.

In order to figure out the mechanism of low-frequency M'' peaks, Arrhenius formula is appealed for analysis. The inset plot in Fig. 8 presents the active energy calculation for the low-frequency peaks in electrical modulus. It was found that the experimental data deviated from the fitting line, suggesting that the response of low-frequency peaks is not exactly a process of thermal activation. But, the active energy of fitting data was still calculated, the value of 0.61 eV is close to the activation energy of 0.538 eV calculated at the grain boundary in Fig. 7, indicating that the additional response in low-frequency modulus is related to the grain boundaries. In other words, there are two kinds of electrical responses related to grain boundaries in pure BCTO ceramics, one is the electrical response dominated by obvious high-frequency modulus peaks and the other is the electrical response related to low-frequency modulus peaks. Therefore, grain boundaries are heterogeneous.

Figure 9 exhibits the temperature dependence of the dielectric constant for YBCTO ceramics at different frequencies. As shown in Fig. 8, a set of clear dielectric peaks above 200 °C can be found for all YBCTO ceramics. For YBCTO ceramics with $x = 0$, 0.10, and 0.20, the dielectric peaks appear at

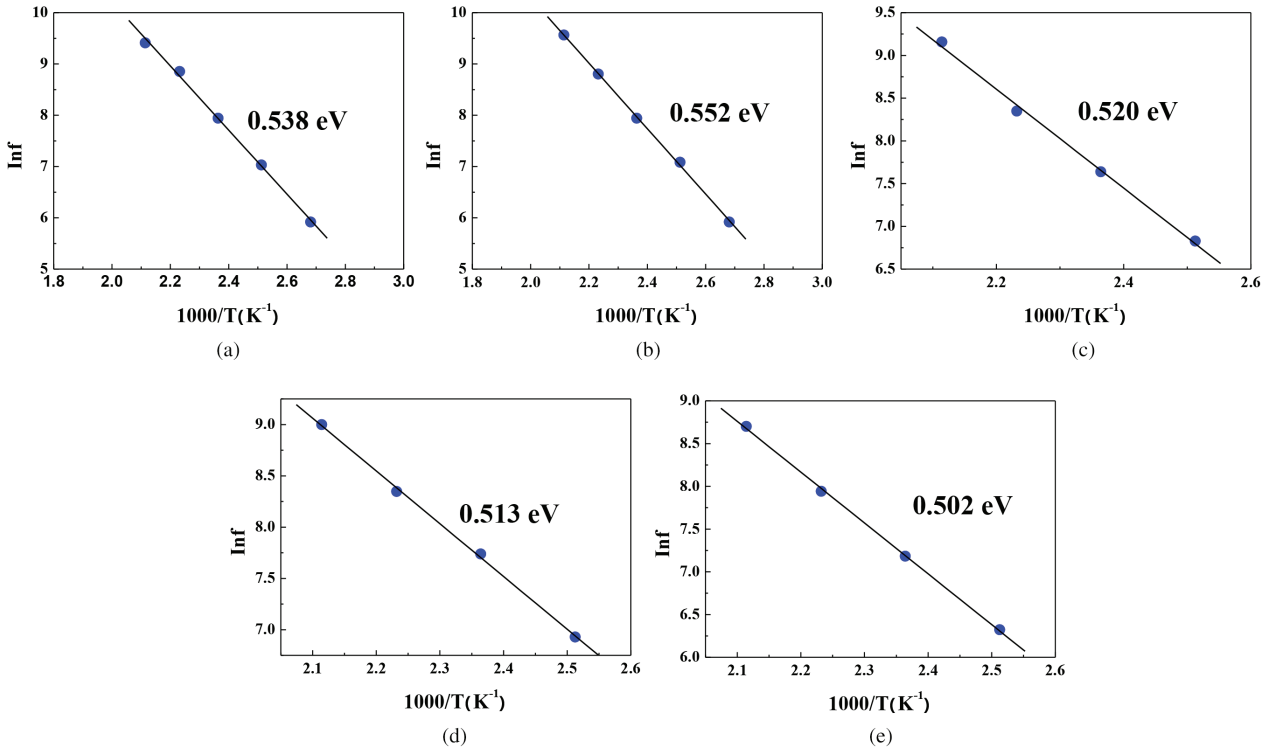

Fig. 7. Arrhenius plots for YBCTO ceramics and the activation energies. (a) BCTO, (b) YBCTO-0.10, (c) YBCTO-0.20, (d) YBCTO-0.25, (e) YBCTO-0.30.

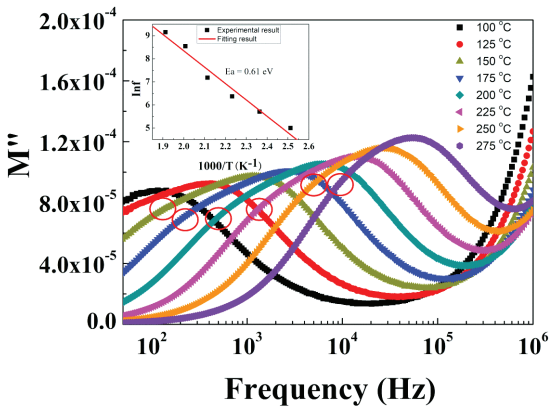

Fig. 8. Frequency dependence of electric modulus and Arrhenius plot corresponding to low-frequency anomaly for pure BCTO ceramics.

~250 °C, while the peaks for ceramics with $x = 0.25$ and 0.30 appear at ~300 °C. The results indicate that Y^{3+} substitution for Bi^{3+} makes this high-temperature dielectric peaks shift to higher temperatures. With the increase of the measuring frequency, the dielectric peak will move to higher temperatures, suggesting a characteristic of relaxation. According to the temperature range where dielectric peaks appear, this set of dielectric peaks is well consistent with the set of electric modulus peaks above 100 °C in Fig. 6. Therefore, the set of dielectric peaks above 200 °C is associated with Maxwell–Wagner relaxation. In addition, if a careful observation is taken, dielectric anomalies at room temperature are observed for Y-doped BCTO ceramics. These anomalies can be systematically studied at lower temperatures, which is beyond our measuring condition.

4. Conclusions

In this work, $(Y_xBi_{1-x})_{2/3}Cu_3Ti_4O_{12}$ ceramics have been successfully prepared by solid-state reaction method. The crystal structure, microstructure, dielectric properties, and complex impedance were systematically investigated. It was found that Y^{3+} substitution for Bi^{3+} has an evidence influence on the microstructure and dielectric properties of BCTO ceramics. XRD analysis confirmed the formation of cubic perovskite phase in solid solution of YBCTO ceramics. SEM micrographs suggested the large abnormal grains were formed in Y-doped BCTO ceramics. $(Y_xBi_{1-x})_{2/3}Cu_3Ti_4O_{12}$ ceramics with $x = 0.20$ exhibited the maximum dielectric constant of ~7400 with a dielectric loss of ~0.055. The investigation of the complex impedance indicated that YBCTO ceramics are electrically heterogeneous. The calculated grains resistances and grain boundaries resistances indicated that the grains are semiconducting and grain boundaries are insulating.

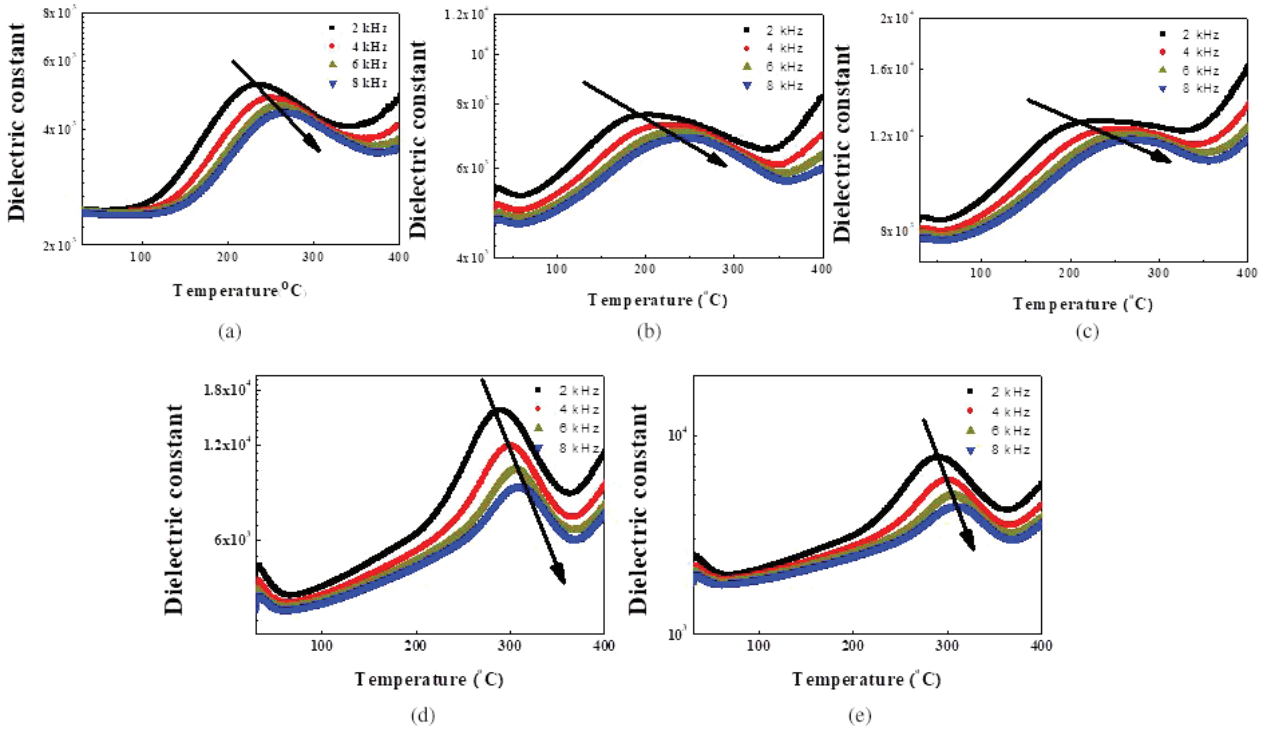

Fig. 9. Temperature dependence of the dielectric constant for YBCTO ceramics. (a) BCTO, (b) YBCTO-0.10, (c) YBCTO-0.20, (d) YBCTO-0.25, (e) YBCTO-0.30.

The activation energies calculated from electric modulus for $(Y_xBi_{1-x})_{2/3}Cu_3Ti_4O_{12}$ with $x = 0.00$, 0.10, 0.20, 0.25, and 0.30 is 0.538 eV, 0.552 eV, 0.520 eV, 0.513 eV, and 0.502 eV, respectively. These values suggested that the low-frequency dielectric constant of $(Y_xBi_{1-x})_{2/3}Cu_3Ti_4O_{12}$ ceramics was attributed to the Maxwell–Wagner relaxation associated with grain boundaries. For pure $Bi_{2/3}Cu_3Ti_4O_{12}$ ceramics, the appearance of additional low-frequency peaks in electrical modulus indicated the grain boundaries are heterogeneous. In addition, a set of clear dielectric peaks above 200 °C can be found for all YBCTO ceramics in the temperature dependence of dielectric constant, which was associated with Maxwell–Wagner relaxation. With Y^{3+} substitution increasing, this set of clear dielectric peaks showed a tendency to shift to higher temperatures. Meanwhile, for ceramics with Y^{3+} substitution, a tiny dielectric anomaly can be observed at room temperature.

Acknowledgments

This work was supported by National Natural Science Foundation of China (NSFC) (Grant Nos. 51902193 and 11974275). The Shaanxi Province Key Science and Technology Innovation Team Project (Grant No. 2019TD-026). Natural Science Basic Research Plan in Shaanxi Province of China (2019JQ-092), the China Postdoctoral Science Foundation (2019M663617 and 2019TQ0191). Scientific Research Plan Projects of Shaanxi Province Education Department (CN) (20JK0755).

References

[1]R. Schmidt and D. C. Sinclair, Anomalous increase of dielectric permittivity in Sr-doped CCTO ceramics $Ca_{1-x}Sr_xCu_3Ti_4O_{12}$ ($0 \le x \le 0.2$), *Chem. Mater.* **22**, 6 (2010).
[2]M. Veith, S. Ren, M. Wittmar and H. Bolz, Giant dielectric constant response of the composites in ternary system CuO–TiO_2–CaO, *J. Solid State Chem.* **182**, 2930 (2009).
[3]M. A. Subramanian, D. Li, N. Duan, B. A. Reisner and A. W. Sleight, High dielectric constant in $ACu_3Ti_4O_{12}$ and $ACu_3Ti_3TeO_{12}$ phases, *J. Solid State Chem.* **151**, 323 (2000).
[4]M. A. Sulaiman, S. D. Hutagalung, M. F. Ain and Z. A. Ahmad, Dielectric properties of Nb-doped $CaCu_3Ti_4O_{12}$ electroceramics measured at high frequencies, *J. Alloys Compd.* **493**, 486 (2010).
[5]S. Kwon, C. C. Huang, M. A. Subramanian and D. P. Cann, Effects of cation stoichiometry on the dielectric properties of $CaCu_3Ti_4O_{12}$, *J. Alloys Compd.* **473**, 433 (2009).
[6]B. S. Prakash and K. B. R. Varma, Effect of sintering conditions on the dielectric properties of $CaCu_3Ti_4O_{12}$ and $La_{2/3}Cu_3Ti_4O_{12}$ ceramics: A comparative study, *Physica B* **382**, 312 (2006).
[7]W. T. Hao, J. L. Zhang, Y. Q. Tan and W. B. Su, Giant dielectric permittivity phenomena of compositionally and structurally $CaCu_3Ti_4O_{12}$ like oxide ceramics, *J. Am. Ceram. Soc.* **92**, 2937 (2009).
[8]J. J. Liu, C. G. Duan, W. N. Mei, R. W. Smith and J. R. Hardly, Dielectric properties and Maxwell–Wagner relaxation of compounds $ACu_3Ti_4O_{12}$ (A = Ca, $Bi_{2/3}$, $Y_{2/3}$, $La_{2/3}$), *J. Appl. Phys.* **98**, 093703 (2005).

[9]M. C. Ferrarelli, T. B. Adams, A. Feteira, D. C. Sinclair and A. R. West, High intrinsic permittivity in $Na_{1/2}Bi_{1/2}Cu_3Ti_4O_{12}$, *Appl. Phys. Lett.* **89**, 212904 (2006).

[10]J. J. Liu, C. G. Duan, W. G. Yin, W. N. Mei, R. W. Smith and J. R. Hardly, Large dielectric constant and Maxwell–Wagner relaxation in $Bi_{2/3}Cu_3Ti_4O_{12}$, *Phys. Rev. B* **70**, 144106 (2004).

[11]Y. Q. Tan, J. L. Zhang, W. T. Hao, G. Chen, W. B. Su and C. L. Wang, Giant dielectric-permittivity property and relevant mechanism of $Bi_{2/3}Cu_3Ti_4O_{12}$ ceramics, *Mater. Chem. Phys.* **124**, 1100 (2010).

[12]Z. Yang, P. F. Liang, L. H. Yang, P. Shi, X. L. Chao and Z. P. Yang, Synthesis, dielectric properties of $Bi_{2/3}Cu_3Ti_4O_{12}$ ceramics by the sol–gel method, *J. Mater. Sci.-Mater. Electron.* **26**, 1959 (2015).

[13]L. H. Yang, X. L. Chao, P. F. Liang, L. L. Wei and Z. P. Yang, Electrical properties and high-temperature dielectric relaxation behaviors of $Na_xBi_{(2-x)/3}Cu_3Ti_4O_{12}$ ceramics, *Mater. Res. Bull.* **64**, 216 (2015).

[14]D. Szwagierczak, Dielectric behavior of $Bi_{2/3}Cu_3Ti_4O_{12}$ ceramic and thick films, *J. Electroceram.* **23**, 56 (2009).

[15]P. F. Liang, Z. P. Yang, X. L. Chao and Z. H. Liu, Giant dielectric constant and good temperature stability in $Y_{2/3}Cu_3Ti_4O_{12}$ ceramics, *J. Am. Ceram. Soc.* **95**, 2218 (2012).

[16]R. Tripathi, A. Kumar, C. Bharti and T. P. Sinha, Dielectric relaxation of ZnO nanostructure synthesized by soft chemical method, *Curr. Appl. Phys.* **10**, 676 (2010).

[17]M. Li, A. Feteria and D. C. Sinclair, Relaxor ferroelectric-like high effective permittivity in leaky dielectrics/oxide semiconductors induced by electrode effects: A case study of CuO ceramics, *J. Appl. Phys.* **105**, 114109 (2009).

[18]Y. H. Lin, J. N. Cai, M. Li, C. W. Nan and J. L. He, Grain boundary behavior in varistor-capacitor TiO_2-rich $CaCu_3Ti_4O_{12}$ ceramics, *J. Appl. Phys.* **103**, 074111 (2008).

[19]P. K. Grubbs, E. L. Venturini, P. G. Clem, J. J. Richardson, B. A. Tuttle and G. A. Samara, Dielectric and magnetic properties of Fe- and Nb-doped $CaCu_3Ti_4O_{12}$, *Phys. Rev. B* **72**, 104111 (2005).